WORLD JOURNAL OF PHARMACEUTICAL RESEARCH
SJIF Impact Factor 8.084
Volume 9, Issue 7, 115-136. Research Article ISSN 2277– 7105

SYNTHESIS AND STRUCTURAL CHARACTERIZATION OF POLYETHERS FROM ISOMANNIDE AND ORGANOTIN DIHALIDES AND THEIR ABILITY TO INHIBIT HUMAN CANCER CELL LINES, ESPECIALLY PANCREATIC CANCER CELL LINE PANC-1

Charles E. Carraher Jr.[1]*, Michael R. Roner[2], Tiasha Arnold[1], Kimberly Shahi[2], Paul Slawek[1], Francesca Mosca[1] and Jessica Frank [1]

[1]Florida Atlantic University, Department of Chemistry and Biochemistry, Boca Raton, FL 33431.

[2]University of Texas Arlington, Department of Biology, Arlington, TX 76010.

Article Received on
03 May 2020,

Revised on 24 May 2020,
Accepted on 14 June 2020,

DOI: 10.20959/wjpr20207-17885

***Corresponding Author**
Charles E. Carraher, Jr.
Florida Atlantic University, Department of Chemistry and Biochemistry, Boca Raton, FL 33431.

ABSTRACT

Polyethers were synthesized from the interfacial polycondensation of isomannide and organotin dihalides with yield increasing as the size of the organotin alkyl group increases. The polymers are of moderate molecular weight ranging from 50 to 230 units in length. Infrared spectral analysis shows the formation of Sn-O bands and absence of the R-OH consistent with polyether formation. MALDI MS shows ion fragments from 3 to 6 repeat units long with good isotopic abundance matches for the presence of tin atoms within the ion fragments. NMR shows the presence of both reactants and the loss of the isomannide protons, as expected. Human cancer cell analysis shows inhibition focusing on the pancreatic cancer line PANC-1 to the picogram/mL for the dimethyltin polymer which is the lowest observed by us. Selected polymers show inhibition of all of the cancer cell lines to the nanogram/mL for breast, lung, colon, prostate and pancreatic cancer cell lines.

KEYWORDS: Organotin polyethers, interfacial polymerization, isomannide, pancreatic cancer, breast cancer, fiber formation, MALDI MS, PANC-1 pancreatic cancer.

INTRODUCTION

We have been involved in the synthesis of a variety of metal-containing polymers. Much of this has been reviewed in a ten volume series [volume 1 in the series][1] and various reviews for platinum,[2-5] organotin,[5-9] Group 5,[10,11] Group 15,[12-14] uranium,[15] ruthenium,[16] and vanadocene-containing[17] polymers. The focus here is on organotin polymers and their ability to inhibit a variety of unwanted organisms including mold, mildew, bacteria, viruses, and here cancer.

Our overall strategy is to couple a known metal moiety, Lewis acid, with known biological activity with a Lewis base that itself has a known biological activity hoping that the combination will have a synergetic effect.

Isomannide (CAS 641-74-7) has a variety of names including the IUPAC name (3*R*,3*aR*,6*R*,6*aR*)-2,3,3*a*,5,6,6*a*-hexahydrofuro[3,2-b]furan-3,6-diol and 1,4-3,6-dianhydro-D-mannitol. Its structure is given in Figure 1.

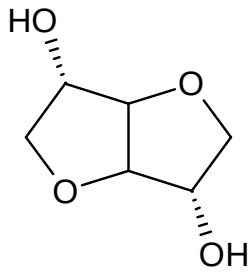

Figure 01: Structure of isomannide.

Isomannide is a natural product originally derived from the secretions of the flowering ash, thus its use is consistent with the idea of "green chemistry" using naturally available feedstocks. It is a heterocyclic compound derived from the double dehydration of hexitols as mannitol and is similar in structure to isoidide and isomannide. It is in fact, an internal ether with hydroxyl groups that are used to form polyethers through reaction with organotin dihalides. There are several techniques to obtain isomannide. Glucose is its main commercial source. Yokoyama and coworkers obtained isomannide from the selective dehydration of mannitol.[18] Biblically it is known as mannitol because of its similarity to the Israelite food for them during their time in the wilderness. Currently, one major interest deals with pancreatic cancer and brain cancer. Clinically isomannide is used to reduce acutely raised intracranial pressure after a head trauma until a more definitive treatment is prescribed.[19,20] It is also used to open the blood-brain barrier by temporarily shrinking the endothelium cells

that make up the barrier. Thus, it is routinely used for delivering drugs to the brain which is an important aspect of our brain cancer efforts.[19-21]

Being composed of two fused rings makes isomannide a rigid structure. It is nontoxic and a green material. This combination makes isomannide a good candidate in condensation polymers. This has been accomplished with the synthesis of polycarbonates and polyesters made from it.[22-30] Cholesteric liquid-crystals have been synthesized using the interfacial polymerization between isosorbide bischloroformate with diphenols.[22] These materials have unusual optical behaviors.

Some of the syntheses with isomannide have employed the interfacial polycondensation of isosorbide bischloroformate with various diphenols.[31-33] Many of these products are cholesteric liquid-crystalline materials with interesting optical properties. The interfacial polycondensation process is the reaction system employed in the present research. The interfacial synthesis was developed by Morgan and coworkers at DuPont and enlarged by Carraher.[34-37] It employs "so-called" high energy reactants such as acid chlorides, here the organotin dihalides, with Lewis bases with an overall activation energy of about 20 kcal/mol. A typical ester-forming reaction between an acid and Lewis acid has an activation of 40 kcal/mol and requires hours of heating. The interfacial process is carried out at room temperature in several seconds to minutes. It is employed commercially in the production of aromatic polyamines used in tire cord and in the production of polycarbonates.[38,39] Because the reactants are commercially available, and the system is industrially known, the production of the materials in gram to kilogram amounts is relatively straightforward.

Here we briefly describe the synthesis of organotin polyethers (Figure 2) from the reaction of isomannide with organotin dihalides, their structural characterization, ability to inhibit cancer cell lines and their ability to form fibers.

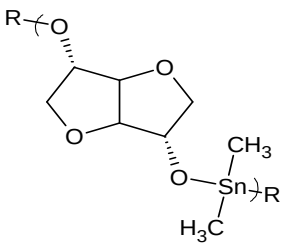

Figure 02: Structure of the repeating unit for the product from reaction of dimethyltin dichloride and isomannide where R represents simple chain extension.

EXPERIMENTAL

Reactions and Reactants: Reactions were carried out using the interfacial polycondensation technique such that the isomannide-containing phase and reaction are maintained under nitrogen because of the instability of isomannide to aqueous base in the presence of oxygen. Briefly, an aqueous solution (30 ml) containing the isomannide (0.00300 mol) and sodium hydroxide (0.0060 mol) was transferred to a one quart Kimax emulsifying jar fitted on top of a Waring Blender (model 1120; no load speed of about 18,000 rpm; reactions were carried out at room temperature, at about 25^{o}C). Stirring was begun and a heptane solution (30 ml) containing the diorganotin dihalide (0.00300 mol) was rapidly added (about 3-4 seconds) through a hole in the jar lid using a powder funnel. The resulting solution was blended for 15 seconds. Dilute (0.1 molar HCl) is added to neutralize any remaining base. The nitrogen blanket is no longer necessary. The precipitate was recovered using vacuum filtration and washed several times with deionized water and heptane to remove unreacted materials and unwanted by-products. The solid was washed onto a glass petri dish and allowed to dry at room temperature.

Diphenyltin dichloride (1135-99-5), isomannide (69-65-8) and dibutyltin dichloride (683-18-1) were purchased from Aldrich Chemical Co., Milwaukee, WS; diethyltin dichloride (866-55-7) was obtained from Peninsular Chemical Res., Gainesville, FL; dioctyltin dichloride (3542-36-7), and dicyclohexyltin dibromide (2954-94-1), dibenzyltin dichloride were obtained from Ventron Alfa Inorganics, Beverly, Mass. The reactants were used as received.

Physical Characterization: Light scattering photometry was carried out employing a Brice-Phoenix Universal Light Scattering Photometer Model 4000. Infrared spectra were obtained employing attenuated total reflectance infrared spectroscopy utilizing a JASCO FT/IR-4100 fitted with an ATR Pro 450-s. Infrared spectra were obtained employing attenuated total reflectance infrared spectroscopy utilizing a JASCO FT/IR-4100 fitted with an ATR Pro 450-s. ^{1}H NMR spectra were obtained in d-6 DMSO employing Varian Inova 400 MHz and Varian 500 MHz spectrometers.

High resolution electron impact positive ion matrix assisted laser desorption ionization time of flight, HR MALDI-TOF, mass spectrometry was carried out employing a Voyager-DE STR BioSpectrometer, Applied Biosystems, Foster City, CA. The standard settings were used with a linear mode of operation and an accelerating voltage of 25,000 volts; grid voltage 90% and an acquisition mass range of 2000 to 100,000. Fifty to two hundred shots were typically

taken for each spectrum. Results employing alpha-cyano-4-hydroxycinnamic acid are included in the present paper. The solid product along with solid matrix were mixed together employing copper spheres giving a fine powder that was employed to obtain the spectra.

Cell Testing: The toxicity of each test compound was evaluated using a variety of cancer cell lines and with human normal embryonic lung fibroblast (WI-38) and mouse embryo-fibroblast (NIH/3T3) cell line as standards. Following a 24 h incubation period, the test compounds were added at concentrations ranging from 0.0032 to 32 microg/mL and allowed to incubate at 37°C with 5% CO_2 for 72 h. Following incubation, Cell Titer-Blue reagent (Promega Corporation) was added (20uL/well) and incubated for 2 h. Fluorescence was determined at 530/590 nm and converted to % cell viability versus control cells.

All cytotoxicity values are calculated against a base-line value for each line that was generated from "mock-treatment" of the normal and tumor cell lines with media supplemented with all diluents used to prepare the chemotherapeutic compounds. For example, if the compounds were dissolved in DMSO and serial dilutions prepared in in Eagle's minimal essential medium, MEM, to treat the cells, then the mock-treated cells were "treated" with the same serial dilutions of DMSO without added chemotherapeutic compound. This was done to ensure that any cytotoxicity observed was due to the activity of the compound and not the diluents. For the studies reported here, the mock-treatment never resulted in a loss of cell viability of more than one percent, demonstrating that the activity observed was not due to cytotoxicity of any of the diluents used, but was due to activity of the tested compounds. When inhibition begins, the slop of the concentration/inhibition curve is steep until total inhibition occurs.

RESULTS AND DISCUSSION

Yield and Chain Length: The yield and chain length are given for the products of organotin dihalides and isomannide in Table 1.

Table 01: Product yield and chain length, degree of polymerization, for the products of isomannide and diorganotin dihalides.

Organotin	Yield (%)	Molecular Weight	Degree Polym.
Dimethyltin	50	2.6×10^4	80
Diethyltin	65	4.4×10^4	120
Dibutyltin	66	2.2×10^4	53
Dicyclohexyltin	98	1.1×10^5	230
Diphenyltin	56	5.7×10^4	130

Yields are generally moderate to good increasing as the alkyl group size increases. Solubility of the polymer appears to be an important factor consistent with the yield trend so that as the alkyl chain length increases, the solubility of the organotin moiety in the organic layer increases allowing for increased growth and increased yield.

The products are low to moderate polymers with chain lengths ranging from 53 for the dibutyltin product to 230 for the dichclohexyltin product (Table 2). There appears to be no trend with respect to chain length with the longest and shortest chains being for similar organotins.

The products are white, as expected since both reactants are either colorless or white.

Infrared Spectral Results: Infrared spectra were obtained for the monomers and polymers. Table 2 contains results of this spectroscopy for the monomers and polymers associated with dibutyltin and diphenyltin polymers. All bands are given in wavenumbers.

Table 02: Infrared spectral bands present in the monomers and polymers associated with the dibutyltin and diphenyltin polymers.

Band Assignment	Isomannide	Bu_2SnCl_2	Bu_2Sn Polymer	Ph_2SnCl_2	Ph_2Sn Polymer
OH St	3402				
CH St Arom				3068,3051	3064,3046
CH Sym St Alip	2992,2958	2960,2927	2963,2953, 2929		2990,2951,
CH Asy St Alip	2891	2872,2858	2871,2856, 2804,2792		2871
SnPh St				1480	1481
CH_3 Sym St		1463	1465		
CH_3 Sym St		1380	1376		
CH_2Scissor	1412		1417		1428
Scissor OH,CH	1197				
Sn-O-C			1014		1022
CO St CHOH	1083		1081		1080
Ring Breath				996	997
CH_3 Rock		878	881		
Sym OP Bend Ring H				729	719
Asy OP Bend Ring H				691	691
SnC Asy St		592	594		
SnC Sym St		509	514		

The absence of the OH stretch in the polymer structures is consistent with bond formation linkage between the organotin moiety and isommanide. Bands are found in the range of 3360

are due to included water. Formation of a new band about 1016 is assigned to the Sn-O-C group is also consistent with linkage between the organotin moiety and isomannide. This band is found at 1014 for the dibutyltin product; at 1022 for the diphenyltin product; 1014 for the dichclohexyl product and 1016 for the dimethyltin product. Presence of bands characteristic of isomannide including various stretch, scissoring, and wagging bands in all polymers is consistent with its inclusion within the polymer structure as are the presence of bands characteristic of the organotin moiety in the polymers. Thus, infrared spectroscopy is consistent with the proposed formation of the organoitn polyether with isomannide. Band assignments from isomannide[40,41] are consistent with those given in the literature as are assignments for the organotin.[42-47]

MALDI MS Analysis: We have been using the solid-state fragmentation of various polymers employing MALDI MS for use in the structural identification of polymers. General MALDI MS analysis of synthetic polymers has been largely unsuccessful because of the requirement that both the matrix and polymer must be soluble in readily volatile liquids that allow intimate mixing of the matrix and polymer. We have employed a modification of this technique that allows MALDI MS to be obtained on non-volatile and insoluble products. This approach has been recently reviewed.[48-50]

MALDI MS spectra were obtained for the monomers and polymers. Three examples are given here. MALDI MS bond cleavage typically occurs at heteroatoms within the polymer backbone.

Figure 3 contains a MALDI MS of the product of diphenyltin dichloride and isomannide. Table 3 contains assignments of the most abundant ion fragment clusters derived from this polymer. Ion fragment clusters to six units are found over the range of 500 to 3,000 Da. The following abbreviations are employed to describe these ion fragment clusters: I for isomannide minus two hydrogens, Ph for phenyl, U for one repeat unit, 2U for two repeat units. Sodium, Na, is a common contaminant.

These regions can be further studied in tabular form comparing the observed relative ion intensities found in the MALDI MS of the samples compared to the relative abundance observed in nature for tin isotopes. Tin has ten isotopes of which seven are present in amounts greater than 5 %. The presence and relative abundance of these isotopes in ion fragment clusters is employed to confirm the presence/absence of tin within the ion fragment

cluster. The relative intensities form a type of "fingerprint" that can be visually identified. Tables 4 and 5 contain such matches for ion fragments containing one and two tin atoms. The agreement with the known relative abundances is reasonable consistent with the presence of tin atoms in the ion fragment clusters.

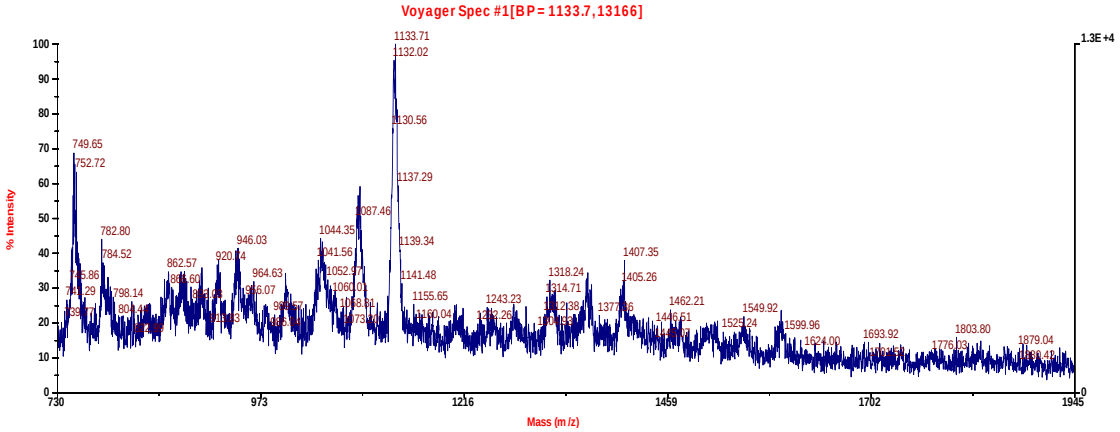

Figure 03: MALDI MS for the product of diphenyltin dichloride and isomannide over the range of 730 to 1945 Da.

Table 03: Major ion fragment clusters for the polymer from diphenyltin dichloride and isomannide over the mass range of 550 to 2900 Da.

Mass, Da	(Tentative) Assignment	Mass, Da	(Tentative) Assignment
586	U+I,Na	1407	3U+I
632	U+SnPh,Na	1544	3U+$SnPh_2$,Na
673	U+SnPh,Na	1563	3U+$SnPh_2$,O,Na
678	U+SnPh	1693	4U+Na
750	U+Sn,I,O	1804	4U+I
784	2U-Ph+O	1978	4U+$SnPh_2$,O,Na
1046	2U-Ph+Na	1993	5U+Na
1134	2U+$SnPh_2$,Na	2518	6U+O
1275	3U+Na	2653	6U+I

Table 04: Isotopic abundance matches for one tin-containing ion fragment cluster containing one tin atom (only ion fragments >5% relative abundance are reported) for the product of diphenyltin dichloride and isomannide.

Known for Sn		U+I,Na	
Da	Rel Abundance	Da	Rel Abundance
116	45	582	48
117	24	583	25
118	75	584	78
119	26	585	25
120	100	586	100
122	14	588	16
124	17	590	18

Table 05: Isotopic abundance matches for two tin-containing ion fragment clusters containing two tin atoms (only ion fragments >5% relative abundance are reported) for the product of diphenyltin dichloride and isomannide.

Known for 2 Sn		U+SnPh, Na		U+$SnPh_2$, Na	
Da	Rel Abund	Da	Rel Abund	Da	Rel Abund
232	12	626	14	667	15
233	13	627	15	668	16
234	43	628	43	669	44
235	35	629	34	670	34
236	94	630	91	671	88
237	51	631	48	672	45
238	100	632	110	673	100
239	35	633	32	674	30
240	81	634	75	675	73
242	32	636	31	677	29
244	22	638	21	679	21

Figure 4 contains the MALDI MS for the dibutyltin dichloride/isomannide polymer. Table 6 contains the major ion fragment clusters to four repeat units. Table 7 contains two isotopic abundance matches for ion fragment clusters found in Figure 4. Agreement is good indicating that these ion fragment clusters contain two tin atoms.

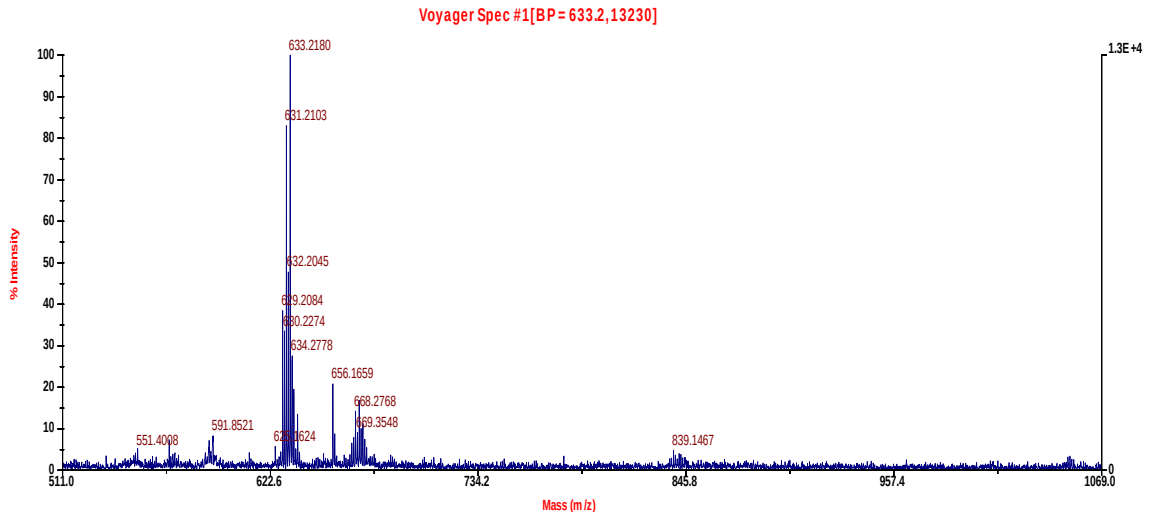

Figure 04: MALDI MS for the product from dibutyltin dichloride and isomannide of the approximate mass range of 500 to1000 Da.

Table 06: Major ion fragment clusters for the product of dibutyltin dichloride and isomannide.

Mass, Da	(Tentative) Assignment	Mass, Da	(Tentative) Assignment
551	U+SnBu	839	2U-Bu+I
592	U+Sn,O,Na	898	2U+I
633	2U-I+Na	987	2U+$SnBu_2$
656	U+Sn,O	1052	2U+Sn,O
670	U+SnBu,I,2O	1131	3U
780	2U+Na	1275	3U+I

Table 07: Isotopic abundance matches for one tin-containing ion fragment cluster containing one tin atom (only ion fragments >5% relative abundance are reported) for the product of dibutyltin dichloride and isomannide.

Known for 2 Sn		2U-I+Na		U+SnBu,I,2O	
Da	Rel Abund	Da	Rel Abund	Da	Rel Abund
232	12	627	11	664	13
233	13	628	12	665	14
234	43	629	42	666	44
235	35	630	33	667	36
236	94	631	91	668	88
237	51	632	51	669	48
238	100	633	100	670	100
239	35	634	35	671	34
240	81	635	78	672	79
242	32	637	31	664	31
244	22	639	21	676	21

Figure 5 is the MALDI MS for the product of diethyltin dichloride and isomannide. Table 8 contains the major ion fragments found for the MALDI MS Figure 5. Table 9 contains the isotopic abundance matches for two ion fragment clusters each containing two tin atoms. The match is reasonable consistent with the clusters containing tin atoms.

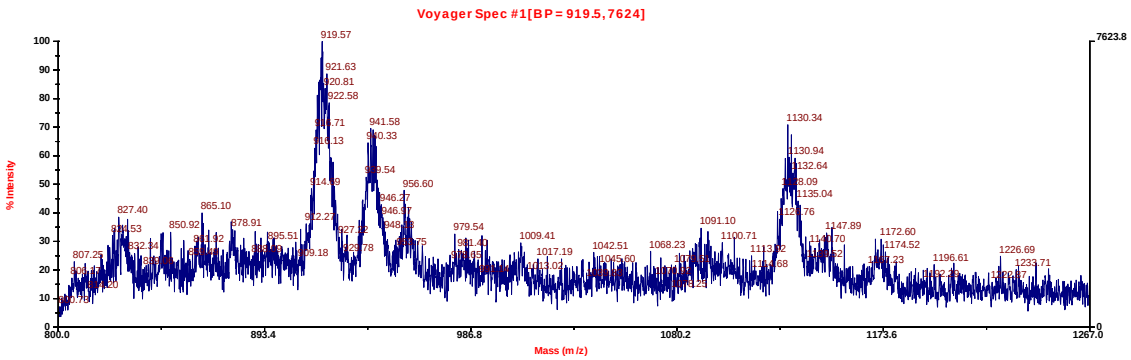

Figure 05: MALDI MS of the product of diethyltin dichloride and isomannide over the mass range of 800 to 1270 Da.

Table 08: Major ion fragment clusters for the product of diethyltin dichloride and isomannide.

Mass, Da	(Tentative) Assignment	Mass, Da	(Tentative) Assignment
537	U+Sn,O,Na	979	3U+O
556	U+Sn,2O,Na	1001	3U+O,Na
577	2U-Et,O	1107	3U+I
593	2U-2Et,O+Na	1130	3U+I,Na
617	2U-O	1150	3U+I,O,Na
633	2U-Et+Na	1268	4U-O
729	2U-2Et+I	1282	4U
919	3U+O	1324	4U+O,Na
941	3U-Et+O,Na	1428	4U+I
967	3U		

Table 09: Isotopic abundance matches for one tin-containing ion fragment cluster containing one tin atom (only ion fragments >5% relative abundance are reported) for the product of diethyltin dichloride and isomannide.

Known for 2 Sn		2U-Et,O		2U-2Et,O+Na	
Da	Rel Abund	Da	Rel Abund	Da	Rel Abund
232	12	571	12	587	11
233	13	572	13	588	12
234	43	573	43	589	45
235	35	574	34	590	33
236	94	575	90	591	89
237	51	576	51	592	51
238	100	577	100	593	100
239	35	578	35	594	35
240	81	579	75	595	76
242	32	581	30	597	31
244	22	583	21	599	22

As in other studies chain breakage occurs at the heteroatoms. The location of preferred chain breakages are depicted in Figure 6.

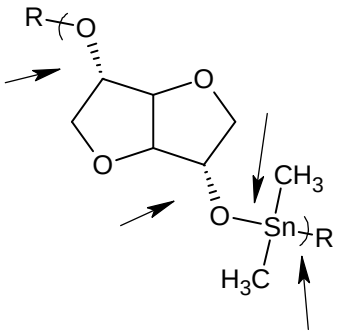

Figure 06: Favored sites for bond breakage in MALDI MS noted by arrows.

NMR Analysis: ^{1}H NMR spectra were taken for all monomers and synthesized compounds. ^{1}HNMR was carried out using d-6 DMSO to dissolve the products. All band locations are given in ppm. The hydroxyl protons on the isomannide found about 7.75 are missing as expected in the polymers.[51,52] Figure 7 contains the NMR for the dibutyltin/isomannide polymer. Isomannide has several protons in varying environments.[51,52] These are given in Figure 8. For the dibutyl polymers these appear about A 4.9; B 4.4; C 4.1.[42-47] In comparison to isomannide itself these bands are at A 4.9; B 4.3; and C 4.1. The locations of the protons on the n-butyltin moiety are a. 1.5; b. 1.6; c. 1.3, and d. 0.86 (Figure 9).[42-47] For the polymer these are found at a. 1.5, b. 1.2, c. 1.1 and d. 0.82. In all cases there are only modest shifts if at all. The other alkyl organotin polymers are similar. For the diphenyltin polymers there are two bands one associated with the ortho position found at 7.3 for the monomer and 7.4 for the polymer and the second one assigned to the meta and para position protons found at 7.9 for the monomer and 7.6 for the polymer.

Because of the poor polymer solubility in d6 DMSO further analysis is not viable.

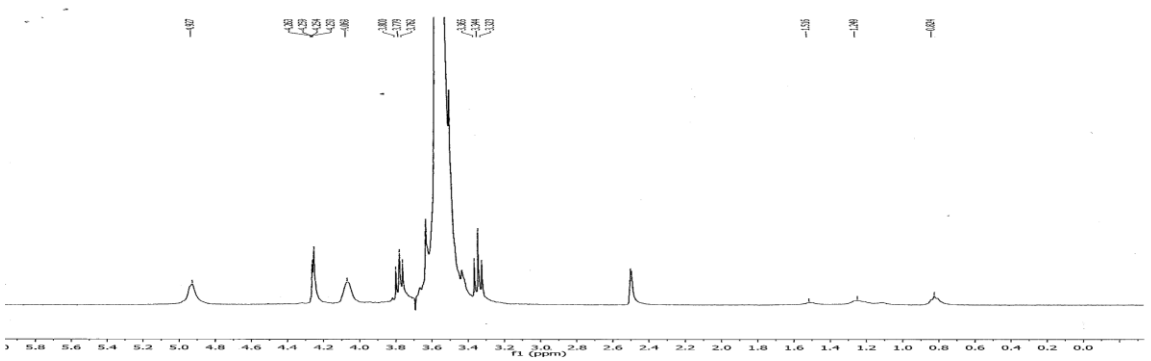

Figure 07: NMR of polymer of dibutyltin dichloride and isomannide.

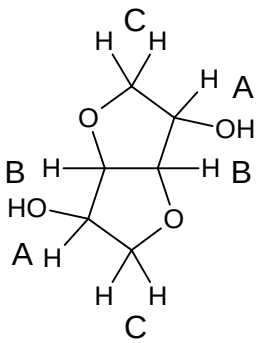

Figure 08: Environmental location of protons associated with isomannide.

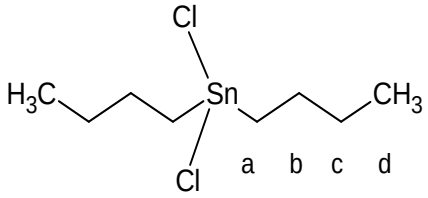

Figure 09: Environmental location of protons associated with the n-butyl group on dibutyltin dichloride.

Cancer Cell Line Analysis: A major purpose in synthesizing metal-containing polymers is to investigate their ability to inhibit unwanted pathogens and infectious agents here the focus is cancer. Table 10 contains the cell lines employed in the current study.

Table 010: Cell lines employed in the current study.

Strain #	NCI Desig.	Species	Tumor Origin	Histological Type
3465	PC-3	Human	Prostate	Carcinoma
7233	MDA MB-231	Human	Pleural effusion breast	Adenocarcinoma
1507	HT-29	Human	Recto-sigmoid colon	Adenocarcinoma
7259	MCF-7	Human	Pleural effusion-breast	Adenocarcinoma
ATCC CCL-75	WI-38	Human	Normal embryonic lung	Fibroblast
CRL-1658	NIH/3T3	Mouse	Embyro-continuous cell line of highly contact-inhibited cells	Fibroblast
	AsPC-1	Human	Pancreatic cells	Adenocarcinoma
	PANC-1	Human	Epithelioid pancreatic cells	Carcinoma

The cells represent a broad range of cancers. Prior studies by us have shown that the active form is the polymeric form and not a degradation product.[9],[53] Isomannide exhibits no inhibition to any of the tested cell lines to the concentration limit tested. Further, cell inhibition is independent of chain length once the chain length reaches twenty or more units.

A number of compounds were recently evaluated with respect to their mode of inhibition.[9] These compounds included polymers derived from various simple diols such as PEG and isomannide and diamines such as histamine, mixed reactant-containing Lewis bases such as salicylic acid and various organotin moieties including dibutyltin, dicyclohexyltin, and diphenyltin employing AsPC-1 cells. This cell line was derived from nude mouse xenografts initiated with cells from the ascites of a patient with cancer of the pancreas.

We were interested in determining if these compounds killed the cells via direct cytotoxicity or by inducing apoptosis. The ApoTox-Glo™ Triplex Assay by Promega was employed in

this study. The assay combines three assay chemistries to easily assess viability, cytotoxicity and apoptosis events in the same cell-based assay well.

All of the compounds killed the target cells by direct cytotoxicity accompanied by the loss of cell membrane integrity and leakage into the surrounding culture medium of a fluorescent substrate. A second, fluorogenic cell-impermeant peptide substrate was used to measure dead-cell protease activity, which is released from cells that have lost membrane integrity. Together these data support the conclusion that the tested compounds killed the tumor cells by disrupting cell membrane integrity.

No changes in caspase -3/7 activity was measured following treatment of these cancer cells with these compounds. This supports the conclusion that induction of apoptosis is not the mechanism associated with the death of these cells.

Two standard cell lines are employed as standards to measure possible effects of the drugs to healthy cell. These are the NIH/3T3 and WI-38 cell lines. The two most widely employed measures to evaluate cell line results are employed in the present study. The initial measure describes the concentration of the drug that inhibits 50% cell inhibition after a specified exposure time. This measure will be described as the effective concentration EC_{50}. Table 11 contains the EC_{50} values for the current polymers and monomers. Values for cisplatin are included. Cisplatin is among the most widely employed chemo drugs in the treatment of a wide variety of cancers. While often effective in treating certain cancers, it produces a wide variety of unwanted side-effects including loss of hearing, numbness, vomiting, kidney damage loss of taste, stomach upset, and loss of hair yet it remains one of the major chemo agents in use today.[54] Because of these unwanted side effects and the observation that chemo treatments become ineffective for many after several rounds of treatment, there is search for other drugs that overcome these limitations. Organotin-containing materials are among agents that are actively being studied as replacements.

The results of the EC_{50} results are striking in that some of the polymers are benign towards many of the cells tested. The lone exception is the PANC-1 cancer cell where the dimethyltin and the dicyclohexyltin polymers show inhibition at very low concentrations, in fact the dimethyltin shows inhibition at the lowest concentration level we have found, in the picogram/mL range. These cell inhibition studies were repeated several times, so we have confidence in them.

Pancreatic cancer has been a recent focus since it has no reported cure. Two pancreatic cancer cell lines are employed in the present study. These are the AsPC-1 cell line which is an adenocarcinoma pancreatic cell line and the PANC-1 cell line which is an epithelioid carcinoma pancreatic cell line. The two tested pancreatic cancer cells are human cell lines widely employed in testing for inhibition of pancreatic cancer. The AsPC-1 cell line represents about 80% of the human cancers found. The PANC-1 represents about 10% of the human cancers detected. Certain of the isomannide organotin polymers show a distinct preference to inhibit the PANC-1 cell line. The dicyclohexyltin polymers also inhibits all the cancer cell lines with the greatest shown toward the PANC-1 pancreatic cancer cell line, here to nanogram/mL level. The reason for the preference and high activity by some of the polymers towards the PANC-1 cell is unknown. The dimethyltin polymer also shows some ability to inhibit all the other human cancer cells most to the nanogram/mL level.

The pair of breast cancer cell lines deserves special comment. They represent a matched pair of cell lines. The MDA-MB-231 (strain number 7233) cells are estrogen-independent, estrogen receptor negative while the MCF-7 (strain line 7259) cells are estrogen receptor (ER) positive. The inhibitions of the two types of breast by the polymers that showed some inhibition were similar. The PC-3 (3465) cells are of interest because this particular cell line is viewed as the most resistant of the prostate cancer cell lines. Again, there was the best inhibition by the dimethyltin polymer, again in the nanogram/mL range.

Table 011: EC_{50} concentrations (micrograms/mL) for the tested compounds. Values given in ( ) are standard deviations for each set of measurements. The EC_{50} values are the concentrations, in micrograms of sample per milliliter of solution, where 50% of the particular cell line, given at the top of each column, are inhibited.

Sample	3T3	*WI-38*	*PANC-1*	*AsPC-1*
Me_2SnCl_2	0.43 (.1)	0.22(.1)	0.80(.1)	0.71(.1)
Me_2Sn/IS	1.0 (.2)	0.00034 (.0001)	.00003 (.00001)	3.7 (.3)
Et_2SnCl_2	0.46(.1)	0.20(.1)	0.48(.1)	0.90(.1)
Et_2Sn/IS	>60	>60	0.44	>60
Bu_2SnCl_2	0.20 (.05)	0.20(.05)	0.0032(.001)	0.012(.01)
Bu_2Sn/IS	>60	>60	>60	>60
Cy_2SnCl_2	0.56(.1)	0.30(.1)	0.85(.1)	0.85(.1)
Cy_2Sn/1S	0.12 (.1)	0.010 (.01)	0.00013 (.0001)	5.6 (.6
Ph_2SnCl_2	0.66(.1)	0.25(.1)	0.71(.1)	0.83(.1)
Ph_2Sn/1S	>60	>60	0.37 (.2)	>60
Isomannide	>60	>60	>60	>60
Cisplatin	0.015(.01)	0.019(.01)	0.0023(.005)	0.0035(.005)

Sample	*PC-3*	*MDA-MB-231*	*HT-29*	*MCF-7*
Me_2SnCl_2	0.51(.1)	0.44(.1)	0.56(.1)	0.66(.1)
Me_2Sn/IS	0.0036 (.001)	0.0015 (.001)	0.0044 (.002)	0.0051(.002)
Et_2SnCl_2	0.61(.1)	0.64(.1)	0.71(.1)	0.77(.1)
Et_2Sn/IS	>60	>60	>60	>60
Bu_2SnCl_2	1.4(1.1)	1.4(1.3)	1.2(.1)	0.7(.06)
Bu_2Sn/IS	>60	>60	>60	>60
Cy_2SnCl_2	0.55(.1)	0.65(.1)	0.65(.1)	0.70(.1)
Cy_2Sn/IS	9.4 (.1)	9.0 (.1)	12 (1)	4.4 (1)
Ph_2SnCl_2	0.82(.1)	0.76(.1)	0.56(.1)	0.68(.1)
Ph_2Sn/IS	>60	>60	>60	>60
Isomannide	>60	>60	>60	>60
Cisplatin	0.0044(.004)	0.0029(.002)	0.0041(.003)	0.0057(.003)

The second measure of the potential effectiveness of the compounds as an anticancer drug is the concentration of compound necessary to inhibit the standard cells compared to the concentration of drug necessary to inhibit the growth of the test cell line. Again, a variety of symbols are employed to describe similar calculations. The term chemotherapeutic index, CI, is employed in the current study. Thus, the CI_{50} is the ratio of the EC_{50} for the NIH/3T3 or WI-38 cells divided by the EC_{50} for the particular test cell. For simplicity, we will simply employ 3T3 to describe the NIH/3T3 cell line.

NIH/3T3 and WI-38 cell lines are most often employed as standards in evaluating the effectiveness of compounds to arrest the growth of tumor cell lines. We have begun comparing the effectiveness of these two cell lines as standards. NIH/3T3 cells are mouse embryo fibroblast cells and are part of a group of cell lines referred to as partially transformed cells in that they are immortal unlike normal cells. They retain other characteristics of normal cells such as being contact-inhibited. Relative to most normal cells they are robust and easily maintained.

By comparison, WI-38 cells are normal embryonic human lung fibroblast cells with a finite life time of about 50 replications. Compared to NIH/ 3T3 cells, they are more fragile and difficult to maintain for long periods of time. Thus, NIH/3T3 cells are often favored because of ease of handling aided by an infinite life span. When there is a difference, values for the WI-38 are generally taken as being more reliable in predicting results for subsequent animal studies. Thus, Table 12 contains CI_{50} values determined employing WI-38 cells.

CI_{50} are given in Table 12. Values calculated as >60/>60 are recorded as simply "-". As the preference found for inhibition of PANC-1, CI_{50} values are large for the dimethyltin,

dicyclohexyltin and diphenyltin polymers showing good preference for inhibiting the cancer compared to the standard cells. With the exception of these, none of the values for the other cell lines were less than one showing no preference for inhibition of the cancer compared to standard.

Table 012: CI_{50} values for monomers and polymers derived from data given in Table 11 based on WI-38 data.

Sample	EC_{50}WI-38/ EC_{50}PNC-1	EC_{50}WI-38/ EC_{50}AsPC-1	EC_{50}WI-38/ EC_{50}PC-3	EC_{50}WI-38/ EC_{50}MDA
Me_2SnCl_2	0.28	0.31	0.43	0.50
Me_2Sn/IS	1.1	0.00009	0.094	0.25
Et_2SnCl_2	0.83	0.81	0.91	0.91
Et_2Sn/IS	>140	-	-	-
Bu_2SnCl_2	63	18	0.14	0.14
Bu_2Sn/IS	-	-	-	-
Cy_2SnCl_2	0.35	0.35	0.55	0.46
Cy_2Sn/IS	>77	0.0018	0.0011	0.0011
Ph_2SnCl_2	0.35	0.31	0.30	0.33
Ph_2Sn/IS	>160	-	-	-
Cisplatin	5.2	3.4	2.7	4.1

Sample	EC_{50}WI-38/ EC_{50}MCF-7	EC_{50}WI-38/ EC_{50}HT-29
Me_2SnCl_2	0.39	0.39
Me_2Sn/IS	0.077	0.067
Et_2SnCl_2	0.71	0.67
Et_2Sn/IS	-	-
Bu_2SnCl_2	0.29	0.17
Bu_2Sn/IS	-	-
Cy_2SnCl_2	0.43	0.46
Cy_2Sn/IS	0.00083	0.0022
Ph_2SnCl_2	0.37	0.45
Ph_2Sn/IS	-	-
Cisplatin	2.1	2.9

In summary, the polymers showed focalized inhibition, mainly towards the PNC-1 pancreatic cancer cells. The inhibition by the dimethyltin was in the picogram/mL the lowest found by us. This polymer also showed inhibition in the nanogram/mL range against all of the cell lines. The cyclohexyltin polymer also showed inhibition towards the PNC-1 at the nanogram/mL level.

SUMMARY

Polyethers were formed in decent amount from the interfacial reaction between isomannide and organotin dichlorides. Product yield increases to about 100% as the alkyl group on the organotin increases in size. MALDI MS shows ion fragments to the range of 3-6 units long with good isotopic abundances matches. The polymers show good inhibition of the tested human cancer cell lines with the greatest inhibition found towards the PNC-1 pancreatic cancer cells to the picogram/mL, the lowest found by us in our testing.

REFERENCES

1. Abd-El-Aziz A, Carraher CE, Pittman C, Sheats J, Zeldin M. Macromolecules Containing Metal-and Metal-Like Elements, A Half Century of Metal-and Metalloid-Containing Polymers, NJ: John Wiley & Sons, 2003; 1.
2. Siegmann-Louda D, Carraher CE. Polymeric platinum-containing drugs in the treatment of cancer; Biomedical Applications, NJ: John Wiley & Sons, 2004.
3. Roner MR, Carraher CE. Cisplatinum derivatives as antiviral agents, Inorganic and Organometallic Macromolecules, NY: Springer, 2008.
4. Carraher CE, Francis A. Water-Soluble Cisplatin-Like Chelation Drugs from Chitosan. J Polym Mater., 2011; 28: 189-203.
5. Roner MR, Carraher CE, Shahi K, Barot G. Antiviral activity of metal-containing polymers organotin and cisplatin-like polymers. Materials, 2011; 4: 991-1012.
6. Carraher CE, Siegmann-Louda D. Organotin macromolecules as anticancer drugs; In Macromolecules Containing Metal and Metal-like Elements, NJ: John Wiley & Sons, 2003.
7. Carraher CE. Organotin polymers in Macromolecules Containing Metal and Metal-like Elements, NJ: John Wiley & Sons, 2004.
8. Roner MR, Carraher CE. Organotin Polyethers as Biomaterials. Materials, 2009; 2: 1558-1598.
9. Carraher CE, Roner MR. Organotin polymers as anticancer and antiviral agents. J Organomet Chem., 2014; 751: 67-82.
10. Carraher CE. Zirconocene and hafnocene-containing macromolecules. In Macromolecules Containing Metal and Metal-like Elements. Vol. 6. Transition Metal-Containing Polymers, NJ: John Wiley & Sons, 2006.
11. Carraher C. Condensation metallocene polymers. *J Inorg Organometal Polyms*., 2005; 15: 121–145.

12. Carraher CE. Organoantimony-containing polymers. J Polym Mater., 2008; 25(1): 35–50.
13. Carraher CE. Antimony-containing polymers. Inorganic and Organometallic Macromolecules, NY: Springer, 2008.
14. Carraher CE, Roner MR, Thibodeau R, Moric-Johnson A. Synthesis, structural characterization, and preliminary cancer cell study results for poly(amine esters) derived from triphenyl-group VA organometallics and norfloxacin. Inorganica Chem Acta., 2014; 423: 123-131.
15. Carraher CE. Uranium-containing polymers. In Macromolecules Containing Metal and Metal-like Elements, 2005; 5. Metal-Coordination Polymers, NJ: John Wiley & Sons, 2005.
16. Carraher CE, Murphy AT. Ruthenium-containing polymers for solar energy conversion. In Macromolecules Containing Metal and Metal-like Elements. Vol. 5. Metal-Coordination Polymer, NJ: John Wiley & Sons, 2005.
17. Sabir T, Carraher CE. Vanadocene-containing polymers. Inorganic and Organometallic Macromolecules, NY: Springer, 2008.
18. Yokoyama H, Kobayashi H, Hasegawa J, Fukuoka A. Selective dehydration of mannitol to isomannide over H□ zeolite. ACS Catal., 2017; 7(7): 4828-4834.
19. Gonzales-Portillo GS, Sanberg P, Franzblau M, Gonzales-Portillo C, Diamandis T, Staples M, Sandberg C, Borlongan C. Mannitol-enhanced, delivery of stem cells and their growth factors across the blood-brain barrier. Cell Transplant, 2014; 23: 531-539.
20. Joshi S, Ergin A, Wang M, Reif R, Yang J, Zhang J, Bruce J, Bigio I. Inconsistent blood brain barrier disruption by intraarterial mannitol in rabbits: implications for chemotherapy. J Neuro-oncology, 2011; 104: 11-19.
21. Carraher CE, Roner MR, Frank J, Mosca F, Slawek P, Miller L. Inhibition of human glioblastomas brain cancer cell lines by metal-containing polymers. World Journal of Pharmaceutical Research, 2019; 8(6): 123-139.
22. Kricheldorf HR, Synthesis of poly(isosoribide carbonate) via melt polycondensation, . J Macromol Sci Rev Macromol Chem Phys., 1997; C37: 599-610.
23. Adelman DJ, Green RN, Putzig DE. US Pat. 6232960, 2003.
24. Adelman DJ, Charbonneau LF, Ung S. US Pat. 6656577, 2003.
25. Kricheldorf HR, Chatti S, Schwarz G, Kruger RP Copolyesters of isosorbide, succinic acid and isophthalic acid: biodegradable, high Tg engineering plastics. J Polym Sci Part A, Polym Chem., 2003; 41: 3414-3424.

26. Lin Q, Pasattie J, Long TE. Synthesis and characterization of chiral liquid-crystalline polyesters containing sugar-based diols via melt polymerization. J Polym Sci Part A, Polym Chem., 2003; 41: 2512-2520.
27. Charbonneau LF, Khanarian G, Johnson RE, Witteler HB, Flint JA. US Pat. 6063495, 2000.
28. Espinosa MA, Galia M, Cadiz Novel flame-retardant thermosets: phosphine oxide-containing diglycidylether as curing agent of phenols J Polym Sci Part A, Polym Chem., 2004; 42: 3516-3526.
29. Hayes RA. US Pat. 6368710, 2000.
30. Sun S, Schwarz G, Kricheldorf HR, Chang T. New polymers of carbonic acid. XXV. Photoreactive cholesteric polycarbonates derived from 2,5-bis(4'-hydroxybenzhylidene)cyclopentanone and isosorbide J Polym Sci Part A. Polym Chem., 2000; 37: 1125-1133.
31. Chatti S, Schwarz G, Kricheldorf, HR. Cyclic and Noncyclic Polycarbonates of Isosorbide (1,4:3,6-Dianhydro-D-glucitol). Macromolecules, 2006; 39: 9064-9070.
32. Collins JR. Br. Pat. 1079686, 1987.
33. Medem H, Schreckenberg M, Dhein R, Nouvestre W, Rudolph H. German Pat. DE 2938464, 1981.
34. Morgan PW. Condensation Polymers by Interfacial and Solution Methods, NY: Wiley, 1965.
35. Millich F, Carraher CE. Interfacial Synthesis, NY: Dekker, 1977.
36. Millich F, Carraher CE. Interfacial Synthesis Vol. II., NY: Dekker, 1977.
37. Carraher CE, Preston J. Interfacial Synthesis NY: Dekker, 1977.
38. Carraher CE. Introduction to Polymer Chemistry FL: CRC Press, 2017.
39. Carraher CE. Polymer Chemistry, 10th Ed. NY: Taylor and Francis, 2018.
40. Bruni G, Berbenni V, Milanese C, Girella A, Cofrancesco P, Bellazzi G, Marini G. Physico-chemical characterization of anhydrous D-mannitol. J Thermal Analysis Calorimetry, 2009; 95: 871-876.
41. Sethu M, Raman M, Ponnuswamy V, Kolandaivel P, Perumal K. Ultrasonic and computational study of intermolecular association through hydrogen bonding in aqueous solutions of D-mannitol. J Mol Liquids, 2007; 135: 46-52.
42. Carraher CE, Roner MR, Crichton R, Moric-Johnson A, Miller L, Black K, Russell F. Synthesis and preliminary cancer cell line results for the product of organotin dihalides

and alpha-cyano-4-hydroxycinnamic acid. J Inorg Organometal Polym Chem., 2016; 26: 1351-1361.

43. Carraher CE, Slawek P, Roner MR, Moric-Johnson A, Miller L, Einkauf J, Russell F. Synthesis and structural and initial cancer cell line characterization of organotin polyesters from dipicolinic acid. J Inorg Organometal Polym Chem., 2016; 26: 1338-1350.
44. Carraher CE, Roner MR, Sooledo N, Moric-Johnson A, Miler L, Johnson J. Synthesis and initial cancer cell results of organotin polyethers derived from the anticoagulant dicumarol. Int J Applied Pharm Biological Res., 2017; 2(5): 1-17.
45. Carraher CE, Roner MR, Campbell A, Moric-Johnson A, Miller L, Slawek P, Mosca F, Einkauf J, Haky J, Crichton R. Synthesis of organotin polyesters from reaction of the salt of D-camphoric ccid and organotin dihalides and initial anticancer activity. J Inorg Organomet Polym Mat., 2018; 28: 481-491.
46. Carraher CE, Roner MR, Patel D, Milller L, Moric-Johnson A, Slawek P, Mosca F, Frank J. Synthesis of organotin polymers from 2-ketoglutaric acid and their ability to inhibit the growth of human cancer cell lines. Hematology Medical Oncology, 2018; 3(1): 1-9.
47. Carraher CE, Roner MR, Lynch M, Moric-Johnson A, Miller L, Slawek P, Mosca F, Frank J. Organotin poly(ester ethers) from salicylic acid and their ability to inhibit human cancer cell lines. Journal of Clinical Research in Onology, 2018; 1: 1-11.
48. Carraher CE, Sabir T, Carraher CL. Fundamentals of Fragmentation Matrix Assisted Laser Desorption/Ionization Mass Spectrometry. NY: Springer, 2008.
49. Carraher CE, Suresh V, Roner MR. Self-matrix activity of organotin polyether ester polymers containing alpha-cyano-4-hydroxycinnamic acid. Journal of the Chinese Advanced Materials Society, 2015; 3: 32-44.
50. Carraher CE, Roner MR, Carraher CL, Crichton R, Black K. Use of mass spectrometry in the characterization of polymers emphasizing metal-containing condensation polymers. J Macromol Sci A., 2015; 52: 867-886.
51. Garaleh M, Yashiro T, Kricheldorf H, Simon P, Chatti S. (Co-)Polyesters derived from isosorbide and 1,4-cyclohexane dicarboxylic acid and succinic acid. Macromol Chem Phys., 2010; 211: 106-1214.
52. Chatti S, Schwarz G, Kricheldorf H. Cylic and noncyclic polycarbonates of isosorbide (1,4:3,6-dianhydro-D-glucitol). Macromolecules, 2006; 39: 9064-9070.
53. Carraher CE, Barot G, Vetter SW, Nayak G, Roner MR. Degradation of the organotin polyether derived from dibutyltin dichloride and hydroxyl-capped poly(ethylene glycol)

in trypsin and evaluation of trypsin activity employing light scattering photometry and gel electrophoresis. Journal of the Chinese Advanced Materials Society, 2013; 1: 1-6.

54. Oun R, Moussa YE, Wheate NJ. Side-effects of platinum-based chemotherapy. Dalton Trans, 2018; 47: 6645-6653.
55. Carraher CE. Fiber forming and thermal properties of polyesters of Group IV B metals. Chem Tech., 1972; 741-744.
56. Carraher CE, Barot G. Polymeric Organotin Fibers, Inorganic and Organometallic Macromolecules: Design and Application, NY: Springer, 2008.